2D Characterization Based on MSGMD And Its Application in Gearbox Fault Diagnosis

Jianqun Zhang
School of Mechanical Engineering
Tongji University
Shanghai, China
zhang_jianqun@tongji.edu.cn

Qing Zhang
School of Mechanical Engineering
Tongji University
Shanghai, China
zhqing@tongji.edu.cn

Xianrong Qin
School of Mechanical Engineering
Tongji University
Shanghai, China
tjqin@tongji.edu.cn

Yuantao Sun
School of Mechanical Engineering
Tongji University
Shanghai, China
sun1979@tongji.edu.cn

2023 IEEE International Conference on Prognostics and Health Management (ICPHM) | 979-8-3503-4625-1/23/$31.00 ©2023 IEEE | DOI: 10.1109/ICPHM57936.2023.10194092

***Abstract*—In recent years, the deep learning-based fault diagnosis method has made remarkable achievements, but it is still challenging in the small sample problem. The image texture features of the vibration signal can effectively represent different gearbox states, which is expected to alleviate the dependence on the number of training samples. Therefore, a new time-frequency diagram characterization method based on multi-symplectic geometric modal decomposition (MSGMD) is proposed. Based on the characterization analysis of multi-component simulation signals, it is proved that the MSGMD time-frequency diagram is feasible to characterize signals, and its advantages over other signal decomposition methods. On this basis, a gearbox fault diagnosis method based on MSGMD and convolutional neural network (CNN) is proposed and applied to solve the small sample problem. The experiment results show that the method can achieve more than 95% recognition accuracy even in dealing with small samples (the average number of training samples for each gearbox state is only 22). Compared with other intelligent diagnosis methods, it gets higher recognition accuracy. The above analysis shows that the proposed method is expected to be used in practical engineering gearbox fault diagnosis.**

Keywords—Multi-symplectic geometric modal decomposition; Vibration signal characterization; Gearbox; fault diagnosis; small sample

I. INTRODUCTION

Once the gearbox failure is not found in time, it is very easy to cause equipment damage, even catastrophic accidents, which will bring huge economic losses. Gearbox fault diagnosis can effectively avoid the occurrence of abnormal downtime and reduce operation and maintenance costs [1]. According to the different technologies used, the current fault diagnosis methods can be divided into traditional fault diagnosis methods and intelligent fault diagnosis methods. Traditional fault diagnosis methods are relying on experienced professionals and skilled workers to observe the time/frequency characteristics of the online data and determine the type of faults. Intelligent fault diagnosis methods can automatically identify the gearbox state of online data through training offline data, and can eliminate the high dependence on professional and technical personnel.

Signal processing technology is an important part of traditional fault diagnosis methods, and it can also be used as the preprocessing technology of intelligent fault diagnosis methods. Common signal processing methods include empirical mode decomposition (EMD) [2], complete ensemble EMD with adaptive noise (CEEMDAN) [3], variational mode decomposition (VMD) [4], symplectic geometric modal decomposition (SGMD) [5, 6], etc. Among them, SGMD can keep the original time feature information unchanged and has good decomposition performance. Existing research and analysis show that MSGMD is superior to EMD and other signal decomposition methods [5, 6]. To solve the two shortcomings of SGMD, i.e., it is easy to ignore low energy components and easy to produce pseudo components under strong background noise, Zhang et al. [7] recently proposed multi-SGMD (MSGMD), and applied it to the separation of gearbox compound fault features, realizing accurate fault diagnosis. They used envelope spectrum to extract fault features, which belongs to the field of traditional fault diagnosis, relying on fault feature frequency to determine gearbox compound faults. At present, the research of MSGMD is still in the initial stage, and its application in intelligent fault diagnosis has not been reported yet.

The intelligent fault diagnosis method based on deep learning has made remarkable achievements because of its strong and adaptive feature extraction. Among many deep learning models, convolutional neural network (CNN) [8-12] is particularly concerned in the field of fault diagnosis. For example, Janssens et al. [8] used one-dimensional (1D) vibration signals to input into the CNN model for fault identification of rolling bearings. To further improve the feature extraction capability of 1D CNN, Wang et al. [9] added a multi-attention mechanism module to the CNN model for rolling bearing fault diagnosis. Compared with 1D CNN, two-dimensional (2D) CNN is more widely used. Most known CNN models need 2D images as input to give full play to their

performance. To apply the advantages of CNN recognition of image to gearbox fault diagnosis, it is necessary to apply the 2D characterization of 1D signals [10, 11]. Typically, based on time-frequency analysis, 1D signals are converted into 2D diagrams to characterize the time-frequency features of signals. In addition, new 2D characterization methods are constantly used in fault diagnosis. The authors of [11, 12] used a gramian angular field (GAF) to convert the vibration signal into an image as the input of CNN. The GAF can be subdivided into the gramian angular summary field (GASF) and the gramian angular difference field (GADF). On the one hand, the research in [11] shows that fault identification accuracy is closely related to the 2D characterization method of signals. On the other hand, the actual number of gearbox samples is relatively scarce, which restricts the engineering application of deep learning-based diagnosis methods. Research in [10] shows that effective 2D characterization of signals can reduce the number of training samples required by network training.

In addition to the characterization of signals, it is also important to select the CNN structure for diagnosis. Typical CNN models such as AlexNet [13] and ResNet18 [14] have been successfully used in image recognition and fault diagnosis. Among them, ResNet18 can effectively mitigate gradient disappearance/explosion, network degradation and other problems by using the residual module.

Considering the above issues, this paper plans to use MSGMD combined with Hilbert transform to generate a time-frequency diagram. Then, the performance of the MSGMD time-frequency diagram used to characterize 1D signals is explored. On this basis, a gearbox fault diagnosis method based on MSGMD and ResNet18 is proposed and applied to solve the small sample problem.

The subsequent organization of the article is described as follows. The second section explains the background knowledge. The third section describes the proposed fault diagnosis method in detail. The fourth section is an experimental analysis. The fifth section gives some conclusions.

II. BACKGROUND KNOWLEDGE

A. Multi-symplectic geometric modal decomposition

On the one hand, in SGMD, the embedding dimension d may only apply to the first separated component and does not apply to other frequency components. To make the embedding dimension match different frequency components, when the first component is removed from the original signal, the remaining signal can be regarded as a new signal. In this way, a new embedding dimension d is selected to reconstruct the trajectory matrix. On the other hand, the original SGMD does not limit the generation of pseudo components under strong background noise. To solve the above problems, the authors of [7] proposed an improved SGMD, namely, MSGMD. The steps of MSGMD mainly include trajectory matrix construction, symplectic geometric similarity transformation, diagonal averaging to obtain the original single component, and merging the single component to obtain the symplectic geometric components (SGCs). The detailed steps of MSGMD can be found in [7]. After MSGMD decomposition, an original signal can be represented by SGCs and the final residual signal $g_{N'}$ as follows.

$$x(t)=\sum_{h=1}^{N'} SGC_h(t)+g_{N'}(t) \tag{1}$$

where $x(t)$ is a vibration signal; $SGC_h(t)$ is the symplectic geometric component of h iteration.

B. ResNet Network

When the depth of CNN is deepening, gradient disappearance/explosion and network degradation are easy to occur. The ResNet takes the residual module as the infrastructure and uses a “short line” to alleviate the above problems. Through this practice, the training speed of the model can be greatly increased and the training effect of the model can be improved.

$$\boldsymbol{x}^{l}=\sigma\left(F(\boldsymbol{x}^{l-1})+\boldsymbol{x}^{l-1}\right) \tag{2}$$

where l is the number of a module; σ is the activation function, generally using the Relu$(\cdot)$ function; $\boldsymbol{x}$ is input; $F(\boldsymbol{x})$ is the feature learned by the general network module.

Based on the above background knowledge, we first study the two-dimensional characterization capability of MSGMD in the next section, and then propose a fault diagnosis method based on the MSGMD time-frequency diagram.

III. THE FAULT DIAGNOSIS METHOD

A. MSGMD time-frequency diagram

After MSGMD decomposition, the corresponding time-frequency diagram can be obtained based on Hilbert transform (HT). Briefly describe the process of obtaining a time-frequency diagram of a signal as follows. For time series $x(t)$, its Hilbert transform result $y(t)$ can be described by the following formula.

$$y(t)=\frac{1}{\pi}P\int_{-\infty}^{\infty}\frac{x(\tau)}{t-\tau}\mathrm{d}\tau \tag{3}$$

where P is the Cauchy principal component.

Based on the HT process, $x(t)$ and $y(t)$ can form a complex signal $Z(t)$.

$$Z(t)=x(t)+\mathrm{i}y(t)=a(t)\mathrm{e}^{\mathrm{i}\theta(t)} \tag{4}$$

where $a(t)=\sqrt{\left[x^2(t)+y^2(t)\right]}$; $\theta(t)=\arctan\left(y(t)/x(t)\right)$.

The instantaneous frequency $\omega(t)$ can be obtained by the derivation of $\theta(t)$.

$$\omega(t)=\frac{\mathrm{d}\theta(t)}{\mathrm{d}t} \tag{5}$$

where $\omega(t)$ is a single valued function of time t, that is, a certain time corresponds to a certain frequency.

The instantaneous frequency corresponding to all component signals $\omega_j(t)$ and instantaneous amplitude $a_j(t)$ is time variables, which can form a three-dimensional time-frequency spectrum of time, frequency and amplitude $H(\omega, t)$. For convenience, the time-frequency diagram obtained above is called MSGMD diagram.

To explore the time-frequency characterization capability of the MSGMD diagram, the following composite signal $x(t)$ is constructed. The signal is composed of component signal $x_1(t)$ and component signal $x_2(t)$.

$$\begin{cases} x(t)=x_1(t)+x_2(t) \\ x_1(t)=\left(1+0.5\sin\left(10\pi t\right)\right)\sin\left(260\pi t-50\pi t^2\right) \\ x_2(t)=0.6\cos\left(80\pi t\right) \end{cases} \tag{6}$$

where $x(t)$ is the constructed composite signal; $x_1(t)$ is frequency conversion amplitude modulation signal; $x_2(t)$ is the cosine signal. The HT diagram of signal $x(t)$ and two components is shown in the figure below.

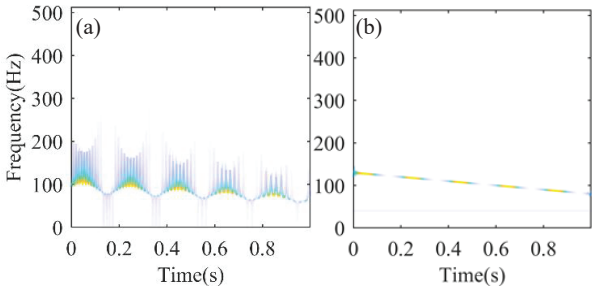

Fig. 1. Time-frequency diagram of simulation signal based on HT: (a) composite signal; (b) component signal

As shown in Fig. 1(a), the frequency components cannot be identified in the composite simulation signal based on HT. In Fig. 1(b), the time-frequency diagram obtained based on HT component signal can clearly show $x_1(t)$ and $x_2(t)$. Fig. 1 shows that the time-frequency diagram based on HT can depict the time and frequency relationship of the signal, but it requires a single component of the input signal rather than a composite signal.

For practical engineering signals such as gearbox vibration signals, single component signals can be obtained by mode decomposition methods such as MSGMD. To highlight the advantages of the MSGMD diagram, EMD, CEEMDAN and VMD are used to analyze the simulation signal for comparison. The parameters set of CEEMDAN and VMD are as follows. In CEEMDAN, the standard deviation of the noise is 2, the average number of times to signal is 500, and the maximum number of filtering iterations is set to 5000. In VMD, the number of component signals is set to 2, and the penalty item is set to 2000. After signal decomposition, MSGMD obtains three components in total, and the first two component signals are analyzed. EMD and CEEMDAN obtain 3 and 10 component signals respectively (residual signals are not used as component signals). The time-frequency diagrams obtained by the four methods are as follows.

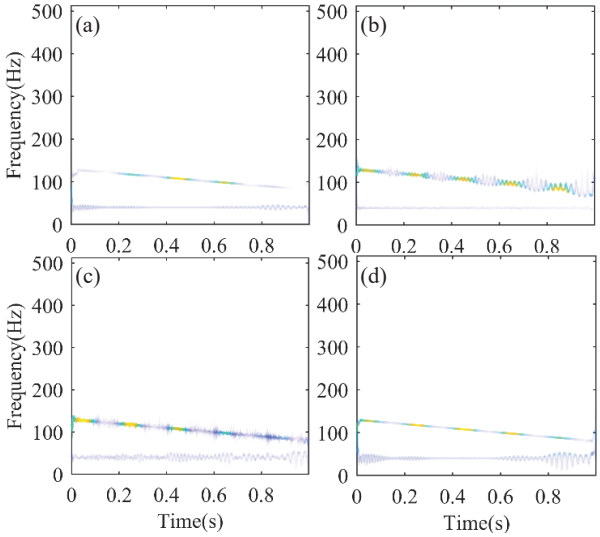

Fig. 2. Time-frequency diagram based on HT: (a) MSGMD component; (b) EMD component; (c) CEEMDAN component; (d) VMD component

It can be seen from Fig. 2 that the MSGMD diagram is closer to Fig. 1(b) than the time-frequency diagram of the other three methods, which can accurately depict the two component signals. The reason is that MSGMD adopts symplectic geometric similarity transformation, which can protect the structural information of the original signal. At the same time, the problem of "end effect" appears in the four decomposition methods. The EMD time-frequency diagram can well display the frequency component of 40 Hz, but it cannot well display the frequency components of variable frequency. Contrary to EMD diagram, VMD diagram can well display component signals of variable frequency components, but cannot well display the component with a frequency of 40 Hz.

To further explore the time-frequency characterization ability of MSGMD for noisy signals, add "-2 db" white Gaussian noise to (6). The time-frequency diagram of the noisy signal obtained by using four decomposition methods is shown in Fig. 3.

Fig. 3 shows that MSGMD has better characterization ability than EMD, CEEMAN and VMD under strong background noise. Only MSGMD can observe the real time-frequency characteristics of the noisy simulation signal, which is specifically shown by the two component signals in the time-frequency diagram of MSGMD. Fig. 3(b) and Fig. 3(c) show the time-frequency plots of EMD and EEMD respectively. The strong background noise completely covers the two component signals. Although Fig. 3(d) is cleaner than Fig. 3(b) and Fig.

3(c), it is unable to depict two component signals. Instead of forming an aggregated frequency line, it fluctuates violently with time transformation.

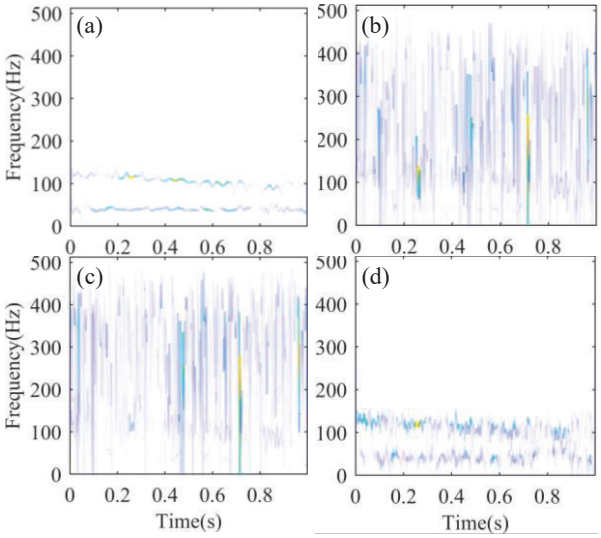

Fig. 3. Time-frequency diagram of the noisy signal based on HT: (a) MSGMD component; (b) EMD component; (c) CEEMDAN component; (d) VMD component

The following inferences can be drawn from Fig. 3.

(1) MSGMD can separate the noise mixed into the signal to the residual signal due to the noise separation conditions set, and can characterize the signal with strong background noise.

(2) EMD and CEEMDAN cannot separate noise, but treat noise as a component signal, resulting in that they are not suitable for time-frequency characterization of signals with strong background noise. VMD can achieve a certain noise reduction effect by setting the correct number of component signals, but the component signal obtained by VMD also contains noise.

B. The proposed MSGMD-ResNet18 method

The last subsection shows that the MSGMD diagram can effectively characterize the time-frequency domain information of 1D signals. Based on the above analysis results, this subsection proposes a gearbox fault diagnosis method combining the MSGMD diagram with ResNet18 network (MSGMD-ResNet18), and its process is shown in Fig. 4.

According to Fig. 4, the steps of the proposed MSGMD-ResNet18 method are as follows.

Step 1: Use the acceleration sensors to collect the gearbox vibration acceleration signals.

Step 2: Use the MSGMD in Section II to decompose the collected vibration signals to obtain several component signals.

Step 3: Use the Hilbert transform in the last subsection to obtain the MSGMD diagrams of the vibration signals.

Step 4: Train the ResNet18 model using MSGMD diagrams obtained from various offline fault history data to obtain a trained fault classification model.

Step 5: Collect online data, transform it into MSGMD diagrams, input it into the classification model trained in step 4, and obtain the diagnosis results.

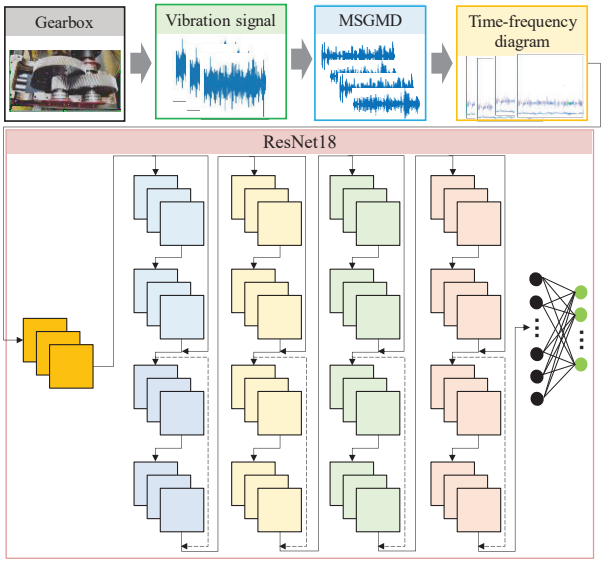

Fig. 4. The Flowchart of the proposed method

Based on the diagnostic steps of the proposed method, we test the effectiveness of the proposed method in the next section.

IV. EXPERIMENT ANALYSIS

A. Data description and diagnosis results

To prove the effectiveness of the proposed method, the method is tested using the open gearbox dataset [15] provided by the University of Connecticut (UoC). The authors of [16] tested seven illustrious datasets based on the four-class benchmark deep learning model, which shows that the UoC dataset is the most difficult to diagnose. The UoC gearbox dataset includes 9 different gearbox states, which are collected from a two-stage parallel shaft gearbox test bench. The fault gear is located on the input shaft of the first stage. The length of the collected signal is 3600, and the corresponding sampling frequency is 20 kHz. The vibration signals of these nine states are used for testing, including normal, tooth missing, tooth root crack, tooth surface spalling and tooth tip defect (including five different fault levels, level 5 represents the lightest degree, on the contrary, level 1 represents the heaviest degree). The sample label and the corresponding quantity of each gear state are shown in Table I.

TABLE I. DIFFERENT GEAR STATES WITH LABELS

Label	Gear states	The number of samples
1	Normal	104
2	Tooth missing	104
3	Tooth root crack	104
4	Tooth surface spalling	104
5	Tooth tip defect_5	104
6	Tooth tip defect_4	104
7	Tooth tip defect_3	104
8	Tooth tip defect_2	104
9	Tooth tip defect_1	104

According to Table I, there are 936 samples in total. The current test is mainly to prove the effectiveness of the proposed method. The training set, verification set and test set are 55%, 15% and 30% respectively. In subsection *C*, tests will be carried out with fewer samples to verify the diagnosis ability of the proposed method in dealing with small samples. Conduct training and diagnosis according to the steps of the method proposed in Section III. The image size of the input ResNet18 model is 224×224. The parameters of batch size, learning rate and epoch number of network training are set to 64, 0.001 and 20, respectively. To illustrate the learning ability of this method, t-distributed stochastic neighbor embedding (t-SNE) [18] is used to visualize the features extracted from the last feature extraction layer (before the full connection layer).

The training is completed in the computer environment of Core (TM) i5-10400F CPU, NVIDIA GeForce GTX 1660 Ti. After 147.82 seconds of training, the model verification rate is 99.29%, which shows that the training of the proposed method is efficient and convenient. The model corresponding to this verification rate is tested, and the overall recognition accuracy is 98.58%, which verifies the validity of the proposed method. The diagnosis results are shown in Fig. 5.

Fig. 5(a) is the confusion matrix, indicating that a total of 4 samples are misdiagnosed. Specifically, One tooth missing sample is misdiagnosed as tooth tip defect_3. Two tooth tip defect_4 samples are misdiagnosed as tooth surface spalling and tooth tip defect_3, respectively; 1 tooth tip defect_1 sample is misdiagnosed as tooth tip defect_3. In addition, the recognition accuracy of other gear states is 100%. The above four wrong samples are concentrated in the different fault degree categories of the tooth tip defect. The reason may be that the signal difference of different degrees of tooth tip defect is small, leading to misjudgment of the method. Fig. 5(b) shows the extracted features using t-SNE, indicating that the features extracted by ResNet18 can separate samples of different gearbox states. To eliminate the influence of accidental factors, five training and tests are conducted. The average time of five training sessions is 143.07 seconds, and the average recognition accuracy of five tests is 98.43%, which proves the stability of the method. In addition, the online dataset testing process can be completed in less than 1 second.

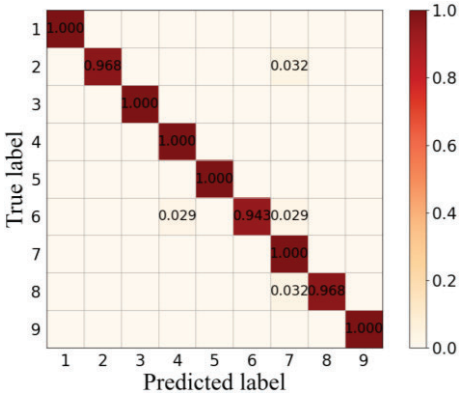

(a) confusion matrix

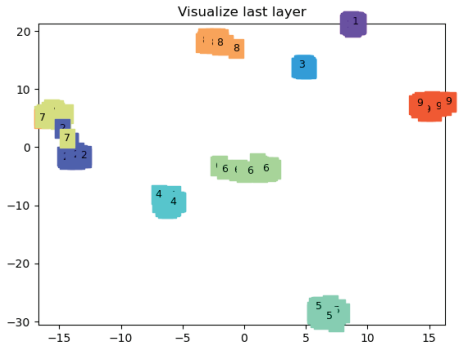

(b) t-SNE dimensionality reduction feature

Fig. 5. Diagnosis results

B. *Comparison analysis*

To prove the superiority of the proposed method, a comparative study of the proposed method is carried out. The comparison mainly includes three parts. The first part is the overall comparison of the methods, that is, the comparison between the recognition results of the proposed method and the results of other references. The second part is the comparison of different inputs, that is, other 2D characterization methods are compared with the MSGMD diagram. The third part is the comparison of ResNet18 network training strategies.

The comparison results between the existing methods in other references and the proposed method are shown in Table II. The full names of these methods can refer to the corresponding literature.

TABLE II. COMPARISON WITH OTHER METHODS

Source	Method description	Quantity	Acc
[15]	Original signal image-local CNN	936	97.57%
	Frequency synchronization analysis-SVM	936	87.48%
[16]	Frequency domain signal-AE	3285	94.95%
	Frequency domain signal-DAE	3285	95.22%
	Frequency domain signal-MLP	3285	95.68%
	Frequency domain signal-LSTM	3285	84.05%
	STFT-AlexNet	3285	47.73%
[18]	Original signal-1DCNN	936	97.5%

	Original signal-ConvRNN	936	96.44%
	Original signal-RNNLSTM	936	93.59%
Ours	MSGMD-ResNet18	936	98.43%

In Table II, the "quantity" represents the sum of all samples. The authors of [16] expanded the number of samples by sliding cutting to meet the training requirements. The average accuracy is the result of 5 times of training and testing. Among the 10 methods provided in the three references, they cover the time domain, frequency domain and time-frequency domain input, as well as 10 different machine learning/deep learning models. It can be seen from Table II that the recognition accuracy obtained by these 10 methods varies from 47.73% to 97.57%, which is less than the recognition accuracy obtained by the proposed MSGMD-ResNet18 method. It proves the advantages of the MSGMD-ResNet18 method in identifying gearbox faults.

Based on ResNet18 network, the comparison results of the MSGMD diagram (the proposed method) and different inputs are shown in Table III.

TABLE III. COMPARISON OF DIFFERENT INPUTS

Inputs	Quantity	Accuracy
Wavelet domain [16]	32850	66.08%
STFT [16]	3285	80.31%
Converting the signal to a 2D matrix [16]	3285	87.34%
GADF	936	90.18%
GASF	936	50.53%
MSGMD diagram	936	98.43%

In Table III, the results obtained from the wavelet domain, STFT and converting the original signal to a 2D matrix are provided by [16]. GADF and GASF are new methods proposed in recent years to convert 1D vibration signals into 2D images, and have achieved good diagnosis results [11, 12]. They are used to compare with the proposed method. The recognition accuracy obtained by these five different inputs fluctuates in the range of 50.53% - 90.18%, which is lower than the recognition accuracy obtained by using the MSGMD diagram. It proves the superiority of the proposed method using the MSGMD diagram as the ResNet18 network input.

The training strategy adopted in this paper is to train ResNet18 network directly. In image recognition, the ImageNet dataset [19] is usually used to assist in the training of the newly constructed network model, to make the network converge quickly and better. Based on the MSGMD diagram input, after using ImagNet to pre-train ResNet18, there are two training strategies for network parameter optimization, i.e., parameter initialization and fine-tuning. The comparison results are shown in Table IV.

TABLE IV. THE COMPARISON OF DIFFERENT TRAINING STRATEGIES

Training strategies	Parameter initialization	Fine-tuning	Training directly
Accuracy	98.29%	85.41%	98.43%

Table IV shows the diagnosis results under three different training strategies. The direct training strategy in this paper is higher than the network parameter initialization and fine-tuning. The reason may be that the characteristics of the ImageNet dataset are different from the MSGMD diagram. That is, the classification model using real-life images cannot provide a reference for training based on MSGMD-ResNet 18. If the MSGMD diagram of other gearboxes is used for training, the diagnosis effect may be improved.

C. *Fault diagnosis results under small samples*

The gearbox fault samples of relatively scarce, mainly due to the extremely short fault time of equipment and the high cost of obtaining fault data labels. To approach the actual gearbox diagnosis, it is necessary to explore the diagnostic performance of the proposed method under a small number of fault samples. The same as the above test, each test is trained five times and tested five times. It should be noted that because of the reduction of training data, there is no verification set except for the training sample proportion of 70%. Fig. 6 shows the diagnosis results of the proposed method under different proportions of training samples.

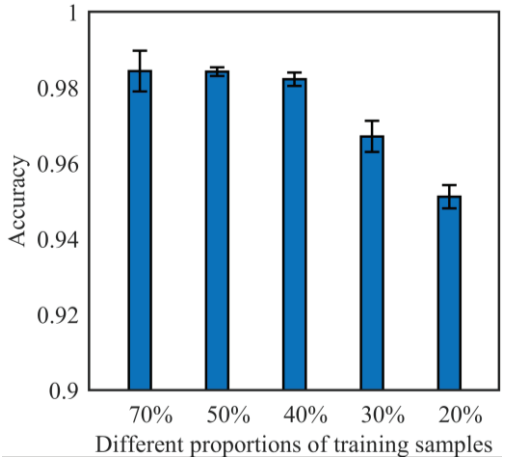

Fig. 6. Diagnosis results of different proportions of training samples

It can be seen from Fig. 6 that the average recognition accuracy of the method will gradually decline with the decrease of the training sample proportion, which indicates that the number of fault samples will affect the recognition accuracy of the method. However, when the sample ratio fluctuates between 20% and 70%, the overall recognition accuracy of the proposed method is still higher than 95%. Specifically, when the proportion of training samples is 70%, 50%, 40%, 30%, and 20%, the corresponding average recognition accuracy is 98.43%, 98.42%, 98.22%, 96.71%, and 95.11%. It shows that the proposed method is robust to the changes in the number of training samples. Even if the training ratio is more than 70%, the recognition accuracy of 11 methods in Table II, Table III and Table IV is still less than 95%. This comparison further highlights the advantages of the proposed method. As mentioned above, when the sample training proportion is 70%, 15% of the data is a verification set, so the diagnosis result is close to the result obtained by training the

sample proportion of 50%. Even if the proportion of training samples is only 20% (the average number of training samples for each gearbox state is only 22), the proposed method can still reach 95.11%, indicating that the proposed method is expected to deal with the small sample problem. The results shown in Fig. 6 further prove that effective 2D characterization of vibration signal is expected to reduce the demand for training samples based on CNN methods.

V. Conclusion

This paper developed a new method based on MSGMD for characterizing 1D signals as 2D images. Based on this analysis, an intelligent fault diagnosis method of MSGMD-ResNet18 is proposed, which uses the MSGMD diagram to solve the problem of vibration signal characterization, and uses ResNet18 network model to solve the problem of effective extraction of features. The effectiveness of the proposed diagnosis method is proved by the experiment analysis. From the comparison results of the whole model, input and training strategies, the proposed method has higher recognition accuracy than the other 17 methods. The specific conclusions are as follows.

(1) The simulation signal analysis shows that the MSGMD diagram is suitable for characterizing 1D signals, and can effectively capture the signal time-frequency information even under the background noise.

(2) The MSGMD-ResNet18 method has the advantages of short training time and high recognition accuracy.

(3) The MSGMD-ResNet18 method is expected to deal with the problem of small samples. Even in the case of small samples, it can accurately identify the gearbox faults.

It is not difficult to find that the fault diagnosis based on small samples is more sensitive to the training set with wrong data. The authors will consider how to conduct small sample fault diagnosis when the training set contains wrong data.

References

[1] Z. Chen, Q. Zhong, R. Huang, Y. Liao, J. Li, and W. Li, “Intelligent fault diagnosis for machinery based on enhanced transfer convolutional neural network,” Journal of Mechanical Engineering, vol. 57, no. 20, pp. 96-105, November 2021. (In Chinese)

[2] N. E. Huang, M. L. C. Wu, S. R. Long, S. S. Shen, W. Qu, P. Gloersen, and K. L. Fan, “A confidence limit for the empirical mode decomposition and Hilbert spectral analysis,” Proc. R. Soc. Lond. A. vol. 459, pp. 2317-2345, September 2003.

[3] L. Li, L. Tang, Q. Ma, Z. Gao, Y. Gao, and Y. Qiao, “CO detection based on photoacoustic spectroscopy with CEEMDAN,” Acta Photonica Sinica, vol. 51, no.11, pp. 1-10, November 2022. (In Chinese)

[4] K. Dragomiretskiy, and D. Zosso, “Variational Mode Decomposition,” IEEE Trans. Signal Process, vol. 62, no. 3, pp. 531-544, February 2014.

[5] H. Pan, Y. Yang, X. Li, J. Zheng, and J. Cheng, “Symplectic geometry mode decomposition and its application to rotating machinery compound fault diagnosis,” Mechanical Systems and Signal Processing, vol. 114, pp. 189-211, January 2019.

[6] Z. Cheng, R. Wang, and H. Pan, “Symplectic geometry mode decomposition method and its decomposition ability,” Journal of Vibration and Shock, vol. 39, no. 13, pp. 27-35, 2020. (In Chinese)

[7] J. Zhang, Q. Zhang, X. Qin, Y. Sun, and J. Zhang, “Gearbox compound fault diagnosis based on a combined MSGMD–MOMEDA method,” Measurement Science and Technology, vol. 33, no. 065102, pp. 1-22, February 2022.

[8] O. Janssens, V. Slavkovikj, B. Vervisch, K. Stockman, M. Loccufie, S. Verstockt, R. V. Walle, and S. V. Hoecke, “Convolutional neural network based fault detection for rotating machinery,” Journal of Sound and Vibration, vol. 377, pp. 331-345, September 2016.

[9] H. Wang, Z. Liu, D. Peng and Y. Qin, "Understanding and Learning Discriminant Features based on Multiattention 1DCNN for Wheelset Bearing Fault Diagnosis," IEEE Transactions on Industrial Informatics, vol. 16, no. 9, pp. 5735-5745, September 2020

[10] J. Zhang, B. Xu, Z. Wang, and J. Zhang. “An FSK-MBCNN based method for compound fault diagnosis in wind turbine gearboxes,” Measurement, vol. 172, no. 108933, pp. 1-11, February 2021.

[11] X. Zhang, M. Zhang, and X. Li, “Rolling bearing fault mode recognition based on 2D image and CNN-BiGRU,” Journal of Vibration and Shock, vol. 40, no. 23, pp. 194-201+207, 2021.

[12] Y. Zhang, W. Liu, H. Gu, A. Alexisa, and X. Jiang, “A novel wind turbine fault diagnosis based on deep transfer learning of improved residual network and multi-target data,” Measurement Science and Technology, vol. 33, no. 095007, pp. 1-11, June 2022.

[13] A. Krizhevsky, I. Sutskever, and G. E. Hinton, “Imagenet classification with deep convolutional neural networks,” Communications of the ACM, vol. 60, no. 6, pp. 84-90, June 2017.

[14] K. He, X. Zhang, S. Ren and J. Sun, “Deep residual learning for image recognition,” 2016 IEEE Conference on Computer Vision and Pattern Recognition (CVPR), Las Vegas, NV, USA, 2016, pp. 770-778.

[15] P. Cao, S. Zhang and J. Tang, “Preprocessing-free gear fault diagnosis using small datasets with deep convolutional neural network-based transfer learning,” IEEE Access, vol. 6, pp. 26241-26253, 2018.

[16] Zhao Z, Li T, Wu J, C. Sun, S. Wang, R. Yan, and X. Chen, “Deep learning algorithms for rotating machinery intelligent diagnosis: An open source benchmark study,” ISA transactions, vol. 107, pp. 224-255, December 2020.

[17] L. V. D. Maaten, and G. Hinton, “Visualizing Data using t-SNE,” Journal of Machine Learning Research, vol. 9, pp. 2579-2605, 2008.

[18] Y. Jin, L. Hou, and Y. Chen, “A Time Series Transformer based method for the rotating machinery fault diagnosis,” Neurocomputing, vol. 494, pp. 379-395, July 2022.

[19] J. Deng, W. Dong, R. Socher, L.-J. Li, K. Li and F.-F. Li, “ImageNet: A large-scale hierarchical image database,” 2009 IEEE Conference on Computer Vision and Pattern Recognition, Miami, FL, USA, 2009, pp. 248-255.